UNIVERSITY OF BRISTOL

Cross, T., De Luca, F., Woods, G. E. D., Giordano, N., Pokhrel, R., & De Risi, R. (2022). FAST-NEPAL: Regionally Calibrated Spectral Method for Reinforced Concrete With Masonry Infills. *Frontiers in Built Environment*, *7*, [689921]. https://doi.org/10.3389/fbuil.2021.689921

University of Bristol - Explore Bristol Research
General rights

FAST-NEPAL: Regionally Calibrated Spectral Method for Reinforced Concrete With Masonry Infills

Theodore Cross*, Flavia De Luca, Gregory E. D. Woods, Nicola Giordano, Rama Mohan Pokhrel and Raffaele De Risi

Department of Civil Engineering, University of Bristol, Bristol, United Kingdom

Reinforced concrete (RC) with masonry infill is one of the most common structural typologies in Nepal, especially in the Kathmandu Valley. Masonry infills are typically made of solid clay bricks produced locally in Nepal. This study aims to calibrate the spectral-based analytical method, namely, FAST, for Nepalese RC-infilled buildings. The FAST method has been initially conceived for Southern European RC buildings with hollow clay brick infills. The calibration is achieved by reviewing code prescriptions and construction practices for RC masonry infills in Nepal and updating the FAST method. The variables of FAST method are calibrated using different information sources and a Bayesian updating procedure to consider the global and local material properties for solid clay bricks. The FAST-NEPAL method obtained is then verified, considering a single school design, for which a detailed state-of-the-art vulnerability assessment is available. Being particularly suitable for large-scale assessment, the method is further validated using data from Ward-35 of Kathmandu Metropolitan City (in the vicinity of Tribhuvan International Airport) obtained from photographic documentation included in a geo-referenced database of buildings collected after the 2015 Nepal earthquake and prepared for census purposes. The comparisons show that the FAST-NEPAL method can be conservative relative to the other data sources for vulnerability and is more accurate at capturing low-level damage. This makes the approach suitable for large-scale preliminary assessment of vulnerability for prioritisation purposes.

Keywords: reinforced concrete, solid clay brick, masonry infills, FAST method, Nepal

INTRODUCTION

In the aftermath of an earthquake event, the speed and efficiency of the first responders are paramount in minimising the loss of human lives. Therefore, authorities should evaluate how vulnerable the infrastructure and residential areas are to seismic events. This can benefit the post-earthquake phase and the preparedness and prevention before seismic events (e.g., Erdik and Fahjan, 2008). This ability is crucial for the developing countries that are more vulnerable to natural disasters due to the limited resources deployed in the aftermath. Seismic vulnerability methods for large-scale risk assessment are essential because they allow the determination of the areas at greatest risk and help assess which areas are most in need of interventions (e.g., World Bank Group, 2016).

The FAST method (De Luca et al., 2014; De Luca et al., 2015) is a rapid method for assessing the vulnerability of reinforced concrete (RC)–infilled buildings on a large scale, up to heavy damage state (DS) (i.e., DS3) according to the EMS-98 scale (Grünthal, 1998). It was applied to Italian and Spanish

earthquake damage data from the recent events occurring in 2009 L'Aquila (Italy), 2011 Lorca (Spain), 2012 Emilia (Italy), and 2016 Central Italy (De Luca et al., 2014; De Luca et al., 2015; Manfredi et al., 2014; De Luca et al., 2017) and compared and improved against refined structural assessment approaches (e.g., Scala et al., 2020). In this study, the FAST method is adapted for the case of Nepalese RC buildings with infills by accounting for the Nepalese building codes (NBC 201, 1994; NBC 2020), local construction practices, and materials for RC-infilled buildings (e.g., Gautam and Chaulagain 2016; Gautam et al., 2016; Brando et al., 2017).

Nepal is an Asian country that occupies one-third of the Himalayas and sits between China and India. Because of the subduction of the Indian tectonic plate beneath the Eurasian plate, it is one of the most seismically active areas globally (Lizundia et al., 2016). The earliest documented event to hit Kathmandu occurred on June 7, 1255; other natural events such as monsoons and floods also significantly affect the population of the country. Nepal has almost 29 million people growing at 1.1% per year (United Nations, 2017). The lack of code enforcement means that there is no reliable standard for quality control of bricks and concrete. The lack of design engineers and expert workmanship means that buildings are often not designed to withstand earthquakes (e.g., Chaulagain et al., 2014a; Lizundia et al., 2016).

RC-infilled buildings are among the most common structural typologies in the urban and semi-rural areas in Nepal, such as the Kathmandu Valley. RC with infills is used for residential, office, and institutional use and has rapidly become prominent over the past few decades (Dizhur et al., 2016). The masonry infill is usually made of solid clay bricks with cement mortar or even mud mortar. These infills are not typically designed to resist lateral loads; however, they can increase the stiffness and, therefore, the natural frequency of the structure.

This study uses the latest Nepalese design codes (NBC 201, 1994; NBC 2020) and local Nepalese material tests (NSET, 2017) to update the FAST method. The other empirical parameters of the method will be adapted to the Nepalese case on the basis of the analytical findings from the recent studies (Chaulagain, 2016a; Scala et al., 2020). The updated FAST-NEPAL method will then be verified, considering, first, a single structure making use of the numerical results from Cross et al. (2020) and, second, it will be applied to a building database of Ward-35 of Kathmandu, and the results will be compared to observed damage from Gorkha (2015).

RC-Infilled Buildings in Nepal

The most common building type used in the urban areas in Nepal is RC-infilled frames, characterised by an RC frame representing the main lateral load-resisting system (considered to be the structural component) and the infill walls made of fired clay bricks. These are typically regarded as non-structural elements but can carry lateral loads (e.g., Kappos, 2000). These walls add to the stiffness of the structure, but they are not modelled explicitly in the conventional finite element analysis for seismic design.

CONSTRUCTION PRACTICES IN NEPAL

According to the World Bank, Nepal is in the list of least developed countries (World Bank, 2020). Its gross domestic product per capita is $1,071, resulting in being the 25th lowest globally. This has a significant impact on the ability of the government to prepare for earthquakes and react in the aftermath of disastrous events. Many buildings in Nepal are constructed by the final owner, who may not follow any building code prescription (see **Supplementary Material, Figure S1A**). Typically, a professional engineer may be involved in designing buildings in the urban areas, but this is only to assist the owner in obtaining the required design permits. Such scenarios occur in the urban areas only. When construction is made in a rural area, the level of control is even lower (Gautam et al., 2016).
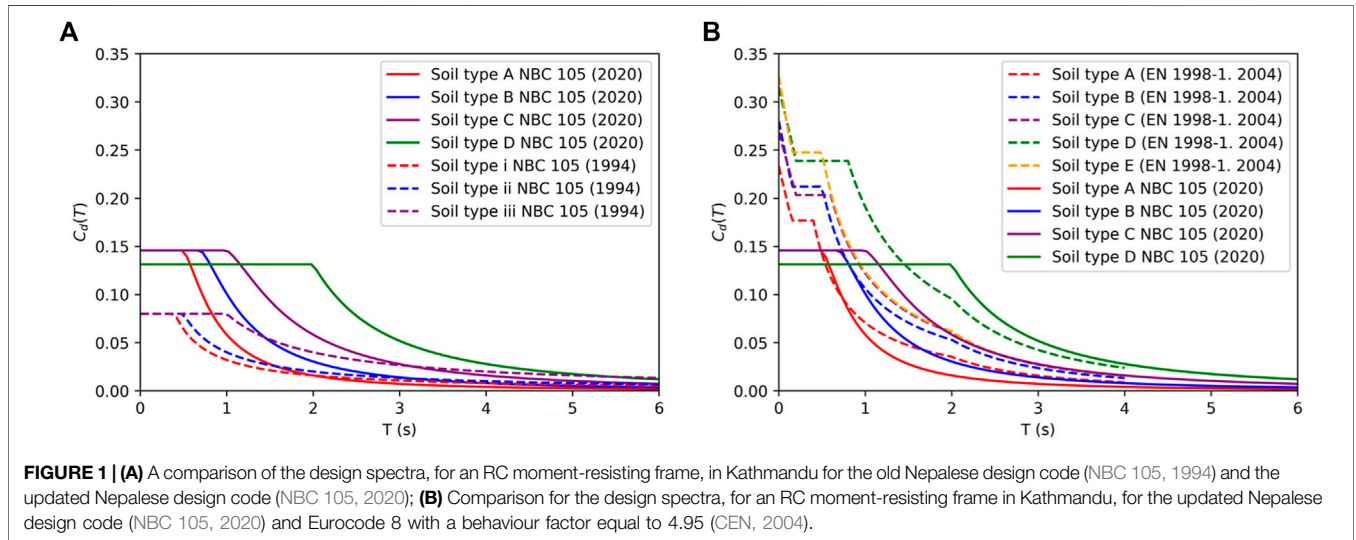
Most of the influence of the design comes from the hired lead contractor, who consults with the homeowner and provides advice on construction. It is typical for the construction of a building to occur in phases (**Supplementary Material, Figure S1B**), with the next storey being added when necessary or when funds become available. This affects the regularity in elevation of the structures; commonly, the lateral load-resisting system is not continuous along the height of the building (**Supplementary Material, Figure S2A**). There are examples of storeys built up with different construction techniques, such as RC with masonry infills on the top of unreinforced masonry (e.g., **Supplementary Material, Figure S2A**). The lack of direct water supplies in some neighbourhoods results in external water tanks sometimes placed in separate dependences close to the building (**Supplementary Material, Figure S2B**) or, most commonly, on the roof terrace (e.g., **Supplementary Material, Figure S2C**).

Although most buildings are rectangular or square, irregular land or design choices may cause structures to be irregular in shape (see **Supplementary Material, Figure S3A,B**). If not adequately considered, then this irregularity can affect the seismic performance of the buildings due to torsional effects. A common feature of Nepalese design is the presence of balconies (see **Supplementary Material, Figure S3C**), which can further complicate the design.

The lack of oversight also leads to other complications. The materials used in construction may not be adequately engineered, and excessive water content in cement causes corrosion of steel reinforcement. Because of the inclined terrain, it is common for building foundations to be stepped or set in an eccentric way to maximise the size of the building. However, as discussed previously, the most critical factors are that most builders do not have any professional experience, and the building owners cannot afford the extra cost of seismic housing. Parajuli et al. (2000) suggest that 98% of builders do not have any professional experience. Consequently, many of the regulations are still unknown or ignored, as shown in **Supplementary Material, Figures S2, S3**, which violate the basic recommendations. There are also examples of mud bricks (instead of fired clay bricks) being used to repair damage to the buildings. Multiple reports (e.g., Build Change org, 2015) state that a significant

TABLE 1 | Soil classification for NBC 105; T_{ci} is the corner period for each ground type.

Type I	Type II	Type III
Rock or stiff soil, sites with bedrock but less than 20 m very stiff cohesive material (>100 kPa) or cohesionless material with standard penetration test values >30	Site unsuitable for Type I or Type III	Ground with a depth of soils greater than those recommended in NBC 105
$T_{c1} = 0.4$	$T_{c2} = 0.5$	$T_{c3} = 1.0$

FIGURE 1 | (A) A comparison of the design spectra, for an RC moment-resisting frame, in Kathmandu for the old Nepalese design code (NBC 105, 1994) and the updated Nepalese design code (NBC 105, 2020); **(B)** Comparison for the design spectra, for an RC moment-resisting frame in Kathmandu, for the updated Nepalese design code (NBC 105, 2020) and Eurocode 8 with a behaviour factor equal to 4.95 (CEN, 2004).

problem in Nepal lies with incorrectly mixed concrete, which can lead to corrosion of steel bars.

Seismic Design Codes

The first of the Nepalese Codes covering RC buildings is the Nepal Building Code (NBC) 201:1994 (NBC 201, 1994); the Mandatory Rules of Thumb for RC buildings, which provides guidance for all stages, from the preliminary investigation to design of the structures and the procurement of materials. This guide is aimed at owner-builders and is designed to offer easy-to-follow advice for safer construction. Examples of the prescriptions given in NBC 201 are to ensure that there are at least two load-bearing walls in each direction for the building, establish standards for the quality of cement used, adequately anchor rebars, and provide straightforward advice for assessing the soil capacity. In terms of materials, "*all cement used shall be Ordinary Portland cement conforming to NS:049–2041, with a cement-sand mix of 1:6 and 1:4 and small quantities of freshly hydrated lime to give plasticity. All bricks used shall be burnt red clay bricks with a size of 240 × 115 × 57 mm with a crushing strength not less than 3.5 N/mm². All walls should have a thickness of at least one half of a brick, but not more than one brick. All mild steel bars should have a strength of 250 N/mm²*" (NBC 201, 1994).

The second code for RC building is NBC 105:1994 (NBC 105, 1994), "Seismic design of Buildings in Nepal", which is a standard of good practice, that acts to supplement the Indian Standard IS 4326 (IS 4326, 1976). This code establishes that the "Seismic Coefficient Method" may be used for any building under 40 m in height, which does not have an irregular configuration, abrupt changes in lateral resistance with height, or unusual size or importance. It also establishes the general principles for ductile design. It states that the structural system must have identifiable

load paths to the ground, be symmetrical, and have uniform storey stiffness and connection to the foundations (NBC 105, 1994).

Furthermore, NBC 105 defines the design spectrum. The design horizontal seismic force coefficient ($C_d(T_i)$) is calculated using the formula shown in **Eq. 1**, where $C(T_i)$ is the ordinate of the basic response spectrum for a translational period (T_i) for each of the soil types described in **Table 1**. In **Eq. 1**, Z is the seismic zoning factor (1.0 for Kathmandu), I is the importance factor for the building (1.0 for residential buildings), and K is the structural performance factor representing the importance of the component to the structural integrity of the building.

$$C_d(T_i) = C(T_i) \cdot Z \cdot I \cdot K \tag{1}$$

The spectral shape for NBC 105 (1994), as shown in **Figure 1A**, is defined on the basis of the soil type. Three soil categories are defined: Type I represents the stiffer (i.e., rock) soil, and Type II and Type III are progressively softer according to the description in **Table 1**. Each soil class is characterised by a corner period (T_{ci}) that affects the spectral shape. **Eq. 2** provides the expression for the design spectra presented in **Figure 1A**.

$$C_d(T_i) = \begin{cases} 0.08, & T(s) < T_{ci} \\ \dfrac{0.08 \cdot T_{ci}}{T(s)}, & T(s) \geq T_{ci} \end{cases} \tag{2}$$

The equation of translational period T_i varies for steel and concrete frames based on **Eq. 3**, where H_i is the height of the central part of the building and k is a coefficient depending on the structural typology (i.e., equal to 0.085 for steel and 0.06 for concrete). This approach is equivalent to the simplified period

formulations available in other seismic codes (e.g., EN 1998–1, 2004).

$$T_i = k \cdot H_i^{3/4} \qquad (3)$$

In 2010, the Nepal Department of Urban Development and Building Construction (UNDP, 2010) released a series of recommendations for improving the earthquake resilience of buildings by enhancing construction practices in addition to design and material advice. This advice includes size and depth of foundations (1,500 mm, set on original soil), positioning, and size of concrete reinforcing bars for beams and columns (minimum overlap distance, locations, examples of beam/column joints reinforcements, standard hooks for stirrups, and a mesh design for concrete slabs). The recommendations also suggested other best design practice rules referring to the international seismic design standards.

In 2020, the Nepal National Building Code for seismic design was updated. This revision includes new conditions for using the "Seismic Coefficient Method" (now referred to as the "equivalent static method"). It also updated the soil type classification criteria. If these conditions are not satisfied, then NBC 105 (2020) suggests a Modal Response Spectrum Method analysis, elastic time history analysis, and non-linear analysis. Elastic time history analysis and non-linear methods are recommended to verify the performance of existing or retrofitted structures. NBC 105 (2020) updates the design spectrum (C_d) for the horizontal base shear coefficient (design coefficient) $(C_d(T_1))$. **Figure 1A** compares the design spectrum for the old Nepalese design code (NBC 105, 1994) and the updated Nepalese design code (NBC 105, 2020). **Figure 1B** shows the design spectra of the updated Nepalese code (NBC 105, 2020) compared with the Eurocode 8 type I design spectrum estimated for the maximum behaviour factor of multi-storey and multi-bay RC moment-resisting frames.

FAST METHOD

FAST (De Luca et al., 2014; De Luca et al., 2015) is a vulnerability evaluation method used for large-scale rapid assessment of RC-infilled buildings, in both the aftermath of a seismic event or to assess vulnerability for preparedness purposes.

The first stage of the FAST method is establishing the approximate Capacity Curve (CC) for a building or a building class. FAST makes the conservative assumption that the damage mechanism of each building is a soft-storey plastic collapse of the ground floor, with the stiff infilled walls failing first and the RC frame undergoing plastic failure later. The CC is calculated considering the contribution of the two materials in parallel. Therefore, the design base shear of RC and the cracking shear strength of the masonry infills (τ_{cr}) must be estimated.
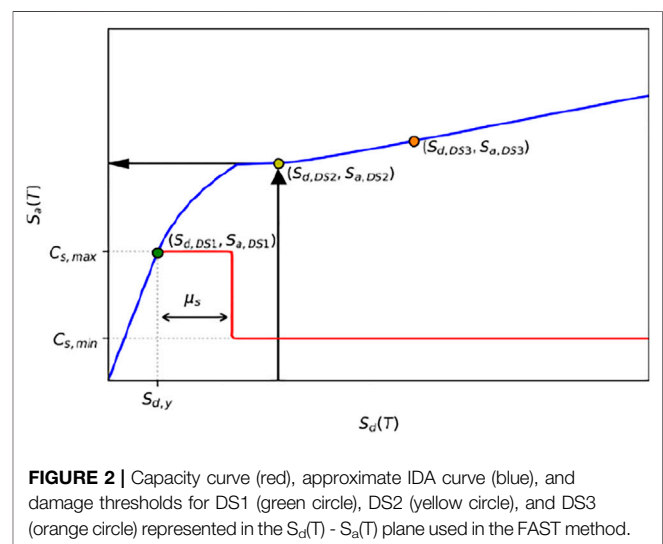
Masonry infills are made from brittle bricks, which, at low peak ground accelerations (PGAs), make the structures very stiff. This stiffness will begin to degrade because of

brittle failure once their maximum shear stress is reached. Once this point is reached, the FAST method assumes no residual strength remains in the walls, and only the RC frame carries the load of the structure. These stages correspond to DS1 to DS3 of EMS-98. The peak shear stress corresponds to DS1, the degradation of infills corresponds to DS2, and the total collapse of the infill walls corresponds to DS3 (see De Luca et al., 2014 and De Luca et al., 2015 for further details). The CC can be represented in the spectral acceleration ($S_a(T)$) versus spectral displacement ($S_d(T)$) plane.

Incremental dynamic analysis (IDA) is an analysis method to estimate the performance of a structure under seismic loading (Vamvatsikos and Cornell, 2002), other methods have since been developed, such as the double impulse pushover (Akehashi and Takewaki, 2019). Having determined the CC curve, it is possible to evaluate the approximate IDA curve. The CC and the IDA curves are related by a strength reduction factor–ductility–period (R–μ–T) relationship (see **Figure 2**).

The attainment of damage thresholds at the first storey can be computed as a function of the inter-storey drift ratio (IDR) of the infills on the basis of experimental results for the typology of infills present in the building or the building class considered. The next step is to convert the IDR into $S_d(T)$. This is done by assuming an approximation of the deformed shape of the structure, depending on the number of storeys present in the building. This is important because one of the main assumptions in the FAST method is that failure of walls occurs at the ground floor. The final stage in the FAST method converts the S_a corresponding to the attainment of each DS into PGA. This allows for comparison with the PGA for the site established from a shake map of the specific location. This can be done using a smooth spectrum (e.g., code spectrum) or a jagged spectrum (e.g., from a recorded time-history).

The FAST method considers contribution of infills, which is one of its advantages over conventional vulnerability analysis

FIGURE 2 | Capacity curve (red), approximate IDA curve (blue), and damage thresholds for DS1 (green circle), DS2 (yellow circle), and DS3 (orange circle) represented in the $S_d(T)$ - $S_a(T)$ plane used in the FAST method.

methods that only consider the contribution of the frame (e.g., Fajfar and Gašperšič, 1996). Although conventional methods are good for identifying the ultimate limit state of a building, they do not accurately represent the stiffness and natural frequency of the infilled structure. This affects significantly the structural response for lower (and more frequent) DSs.

In establishing the contribution of infill walls, it is vital to consider the differences between solid clay bricks and hollow clay bricks. Hollow clay bricks have holes in them to improve their insulating properties. This reduces their horizontal area and, consequently, the ability of the infill to resist shear forces. The IDR damage thresholds for solid brick infills are different from hollow clay brick ones. The FAST method, in the form used so far in the literature (De Luca et al., 2014; De Luca et al., 2015; De Luca et al., 2017; Scala et al., 2020), has been calibrated for use in Southern European countries and their typical hollow clay bricks. A novel adaptation of the method to different regional contexts, such as Nepal, requires new shear values and new IDR thresholds to represent the difference in mechanical properties between hollow and solid clay bricks. Solid clay bricks are typically used in Nepal and represent the standard to which the method has to be adapted.

Capacity Curve

The CC represents the inelastic behaviour of a structure in terms of spectral displacement and spectral acceleration. The main equations used in the FAST method are those for calculating the parameters that define the CC (i.e., $C_{s, max}$, $C_{s, min}$, $C_{s, design}$, and T). These are presented in the following (see **Eqs. 4–7**). The reader should refer to De Luca et al. (2015) and De Luca et al. (2017) for further details. The main variables of the FAST method are kept the same as in previous studies (i.e., De Luca et al., 2015 and De Luca et al., 2017). The variables modified for the Nepal case are IDR for DS1 to DS3 and the τ_{cr} value. For τ_{cr}, the distribution obtained in the following is used. $C_{s, max}$ (**Eq. (4)**) is the inelastic acceleration of the equivalent single degree of freedom (SDOF) at which the maximum strength is obtained (De Luca et al., 2014). $C_{s, min}$ (**Eq. (5)**) is the inelastic acceleration of the equivalent SDOF at the attainment of the plastic collapse mechanism of RC structure (all the infills of the storey involved in the mechanism have attained their residual strength). T is the equivalent period computed from the elastic period T_0 of the infilled building given in **Eq. 7**. In **Eqs. 4, 5**, N is the number of storeys, m is the average mass of each storey normalised by the building area (assumed equal to 0.8 t/m²), λ is a coefficient for the evaluation of the first mode participation mass with respect to the total mass of the multiple degrees of freedom according to Eurocode 8 (CEN, 2004), and ρ_w is the ratio between the infill area (A_w) evaluated along one of the building's principal directions and the building area A_b. The α coefficient accounts for the strength contribution of the RC element at the attainment of the infill peak strength. The β coefficient accounts for the infills residual strength contribution after attaining the peak lateral resistance of the bare RC structure (see De Luca et al., 2014; De Luca et al., 2015). $C_{s,design}$ is the peak design spectrum value for the design spectrum that the structure was most likely designed to. For the Nepal case, this can vary based on the age of the structure.

$$C_{s, max} = \alpha \cdot C_{s,design} + \frac{1.3 \cdot \tau_{cr} \cdot \rho_w}{N \cdot m \cdot \lambda} \qquad (4)$$

$$C_{s, min} = C_{s,design} + \frac{\beta \cdot 1.3 \cdot \tau_{cr} \cdot \rho_w}{N \cdot m \cdot \lambda} \qquad (5)$$

$$C_{s,design} = S_{a,d}(T) \cdot R_\alpha \cdot R_\omega \qquad (6)$$

$$T = \kappa \cdot 0.023 \cdot \frac{H}{\sqrt[2]{100 \cdot \rho_w}} = \kappa \cdot 0.0023 \cdot \frac{H}{\sqrt[2]{\rho_w}} \qquad (7)$$

Many of the assumptions in FAST are conventional for buildings designed in Mediterranean countries and its application to a different regional context requires a bespoke assessment. The R–μ–T relationship considered in FAST is SPO2IDA (for further details, the reader is referred to Vamvatsikos and Cornell, 2006).

Adaptation of FAST Method to the Nepalese Case: "FAST-NEPAL"

Solid clay bricks are the predominant type of brick used in Nepal. As their name suggests, the bricks are made of clay pressed into a mould that is then baked or "fired" to solidify the bricks. As with most types of fired clay, the bricks undergo brittle deformations when their maximum shear stress (τ_{max}) is reached. As deformation of the wall continues, cracks begin to propagate through the wall along mortar boundaries (bed joints), see also EN 1996-3 (2006). For RC-infilled buildings in Nepal, cement mortar is considered because it is most common in Kathmandu (e.g., CBS, 2012; Chaulagain et al., 2015). Kathmandu is the focus in the following analyses; however, in more rural parts of Nepal, mud mortar is more commonly used.

The available ductility of masonry infills (μ_s) has previously been approximated to be 2.5 for Southern European masonry-infilled RC (Manfredi et al., 2012). This value is updated using analytical models of Nepalese masonry buildings. Global data on the cracking shear stress (τ_{cr}) and IDR thresholds for DS1 to DS3 for solid clay bricks were gathered to update the FAST method for its application in Nepal. Then, local data of mechanical properties are collected for the country (NSET, 2017) and used for Bayesian updating of the shear stress. The new properties distributions obtained can be used to carry out the FAST methodology and derive fragility curves for the Nepalese context.

Ductility Assessment

μ_s is defined as the available ductility up to the degradation of the infills relative to the displacement at V_{max}. μ_s is found to be 2.5 (Manfredi et al., 2012) for Mediterranean masonry buildings, typically made of hollow clay bricks. This may not be representative of the available ductility in Nepalese RC with infill structures because they are made of solid clay bricks. An assessment of this parameter for the Nepal context is achieved through a piecewise linear fit to the analytical static pushover analysis in Chaulagain (2016a) to find a more accurate value. In Chaulagain (2016a), several pushover analyses are carried out on various RC buildings with infills; these were summarised in **Supplementary Material, Table S1**. These buildings are a combination of engineered and non-engineered structures. The structures with the irregular top level are not included for the available ductility assessment. Linear
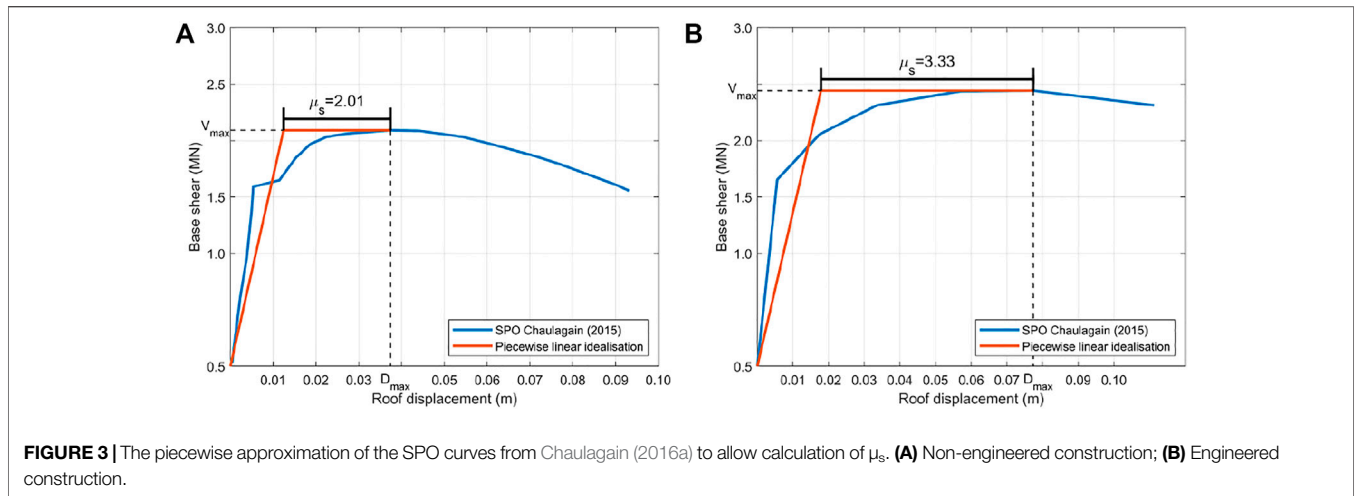
FIGURE 3 | The piecewise approximation of the SPO curves from Chaulagain (2016a) to allow calculation of μ$_s$. **(A)** Non-engineered construction; **(B)** Engineered construction.

interpolation of the initial stiffness is applied using the equal-area (equal-energy) method, whereby the area under the curve and the linear-interpolation are equal at the maximum base shear. This is the method deployed by Eurocode 8 and has a relatively limited error between the curve and piecewise-linear fit (see De Luca et al., 2013). The elastic segment continues until the maximum shear resistance, V_{max}. The horizontal section of the piecewise idealisation continues to the maximum point of the pushover curve, as shown in **Figure 3**. The obtained $μ_s$ values for engineered and non-engineered buildings are 2.01 and 3.33 with an average (2.67) close to the original 2.5 value assumed in previous versions of the FAST method. Such values can be used for engineered and non-engineered building classes, as identified by their year of construction.

Global Data Set

The global shear cracking data set ($τ_{global}$ in the following) was gathered from the MADA masonry database (Augenti et al., 2012) and had a total size of 48 tests (Meli, 1973, Abrams, 1992, Zarri, 1992, Riddington and Jukes, 1994, Zhuge et al., 1996, Andreaus and Moroder, 1991, Yi et al., 2004, Valluzzi et al., 2002; Caliò, 2011). The data for IDR1, IDR2, and IDR3 was gathered from Cardone and Perrone (2015) with the number of tests equal to 14, 12, and 15, respectively. Additional datasets of infills have been recently made available in the literature such as Blasi et al. (2021), but they do not have data for the all three damage states required herein. The data from Cardone and Perrone were fitted with three different distributions (**Figure 4**): normal, log-normal, and Generalised Extreme Value (GEV). In **Supplementary Material, Table S2**, the fitted parameters for the distribution are presented. Because the GEV distribution is a three-parametric distribution and the normal and log-normal are two-parametric distribution, an information criterion accounting for this difference is used to identify the most efficient distribution for the considered data. The Akaike information criteria (AIC) in its basic version, see **Eq. 8**, and in its improved version (AIC$_C$), to account for a limited data sample and to avoid overfitting (**Eq. 9**), are used to rank the different fits (Akaike, 1974). In **Eqs. 8, 9**, k is the number of parameters in the model, L is the maximum likelihood from the fit, and n is the number of samples. AIC$_C$ is suggested for cases where the sample size is fewer than 50 (Cavanaugh, 1997).

$$AIC = 2k - 2\,ln(L) \quad (8)$$
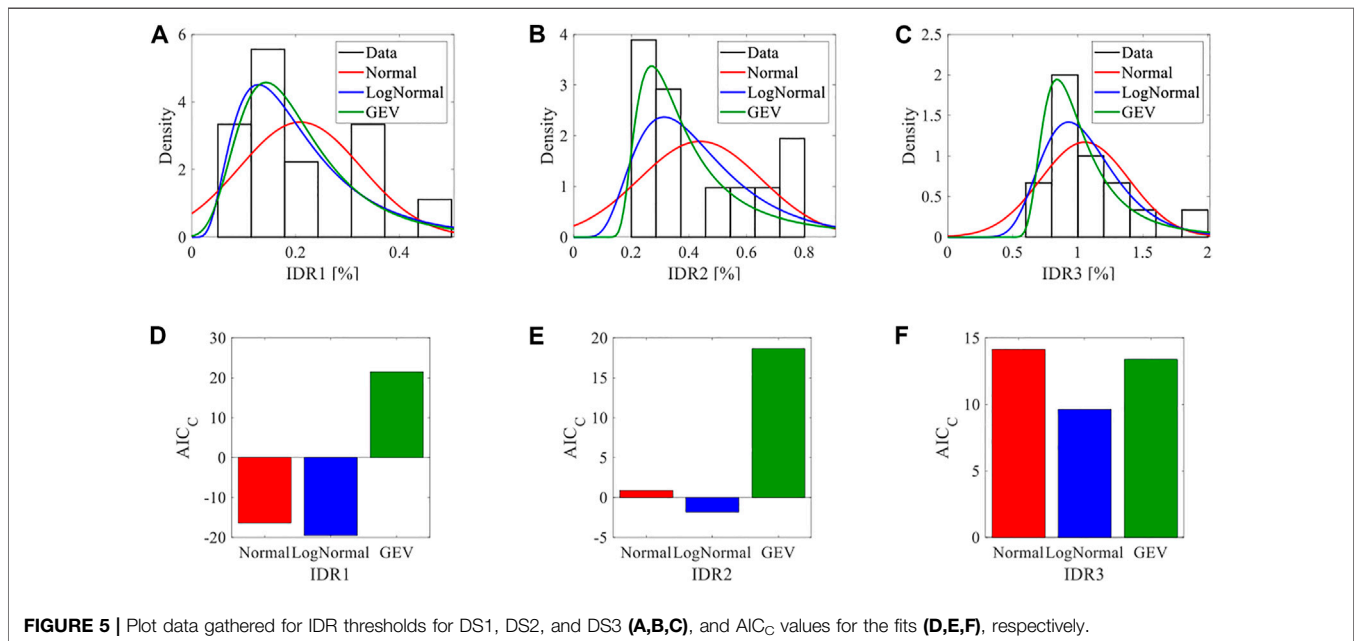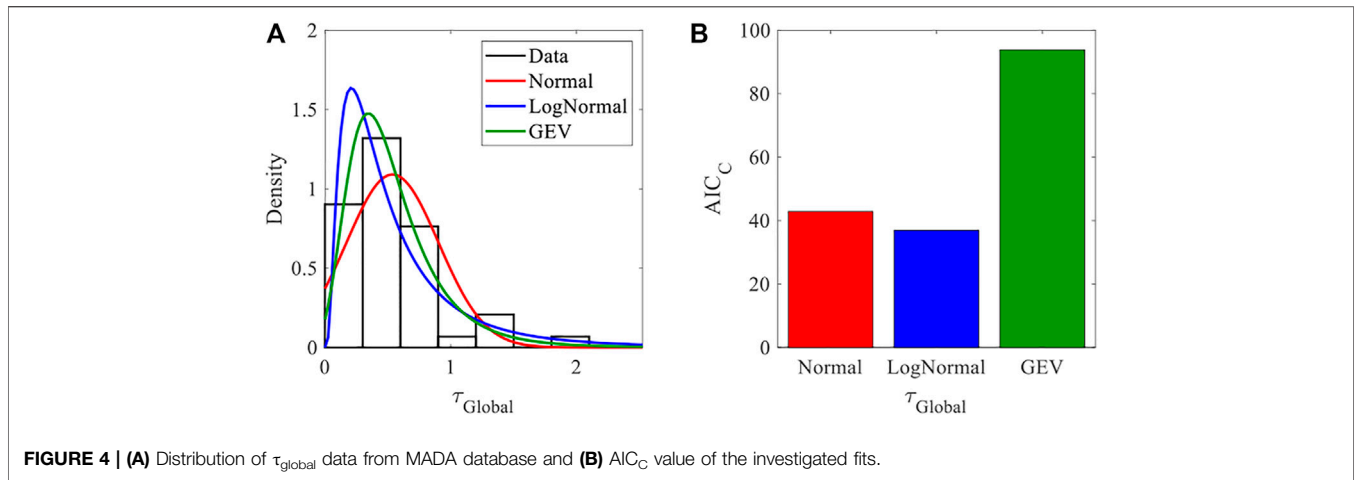
$$AIC_C = AIC + \frac{2k^2 + 2k}{n - k - 1} \quad (9)$$

The AIC$_C$ value was compared for each fit, with the lowest value denoting the most efficient for that data set. For all data sets (**Figures 4, 5**), the AIC$_C$ suggests that the Log-Normal Distribution best represents the Global Data for all the variables considered ($τ_{global}$, IDR1, IDR2, and IDR3). This distribution is commonly used for variable distributions used in earthquake engineering for fragility analysis (e.g., Porter et al., 2007; De Luca et al., 2015).

In particular, the median results can be compared with those calibrated in De Luca et al. (2015) for hollow clay brick infills (i.e., $τ_{Cr} = 0.4$ MPa; IDR1 = 0.1%, IDR2 = 0.4%, and IDR3 = 0.8%). The median value obtained for IDR2 in **Supplementary Material, Table S2** (i.e., IDR2 = exp (−0.9299) = 0.39%) is very similar to the value obtained in the calibration for hollow clay bricks (De Luca et al., 2015). For the case of IDR1 and IDR3, the difference is more significant (i.e., IDR1 = exp (−1.7158) = 0.18%, IDR3 = exp (0.010) = 1.01%) with the values for solid clay bricks being larger. The logarithmic standard deviations obtained for IDR1, IDR2, and IDR3 are lower with respect to the value suggested by Colangelo (2012) (i.e., 0.60, 0.67, and 0.47) for hollow clay brick infills and used in previous applications of FAST method (see De Luca et al., 2015).

The $τ_{cr}$ value for De Luca et al. (2015) and the global data set of solid clay bricks are very similar, with the median obtained in this study being only slightly larger (i.e., $τ_{global}$ = exp (−0.8797) = 0.415 MPa). This similarity can be explained by the fact that the mortar is the limiting factor for the cracking shear stress and not the bricks type, as suggested in many codes (e.g., EN 1996-3, 2006).
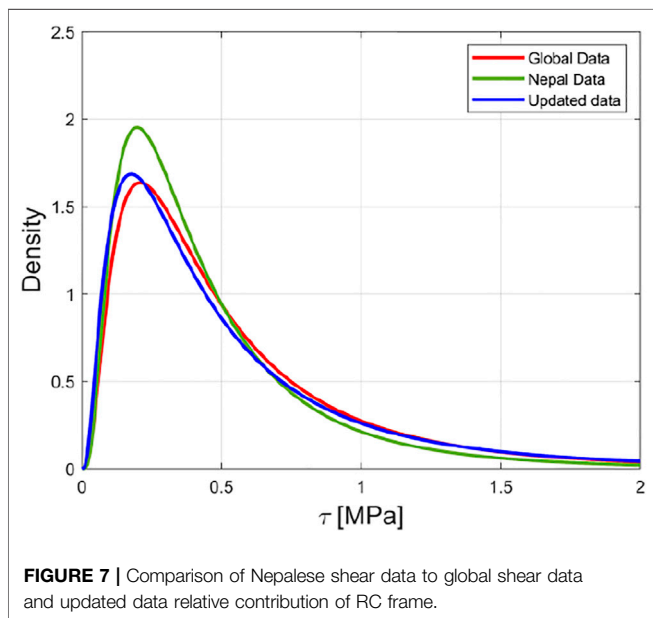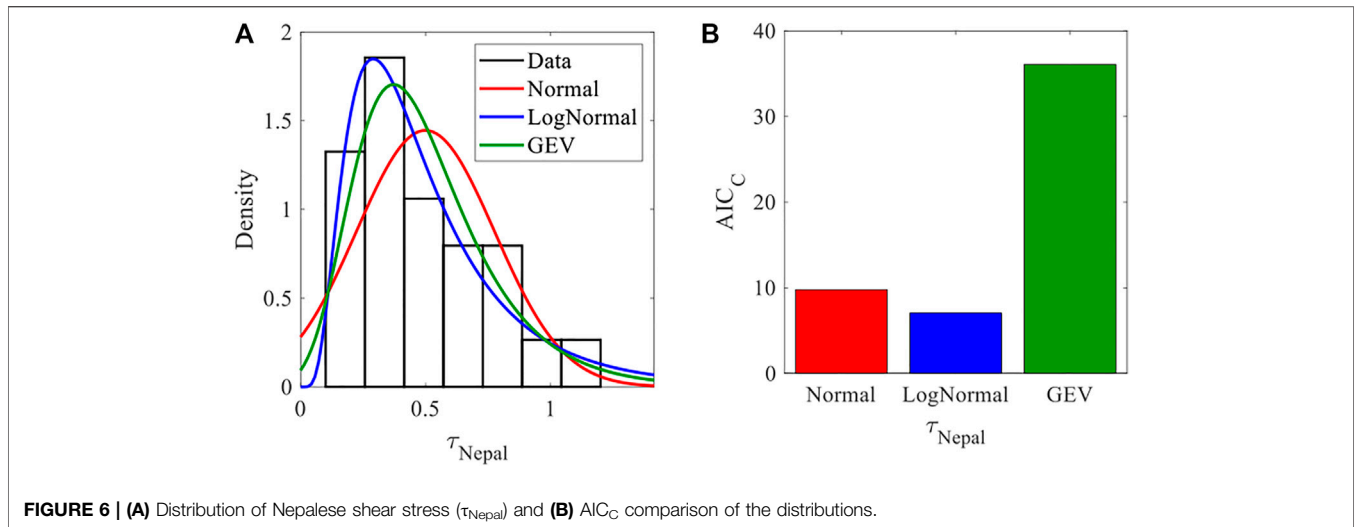
Nepal Data Set and Bayesian Updating

For the FAST method to be reliably used to analyse data in Nepal, it would be ideal to have regional data for all the variables.

FIGURE 4 | (A) Distribution of τ_{global} data from MADA database and **(B)** AIC$_C$ value of the investigated fits.

FIGURE 5 | Plot data gathered for IDR thresholds for DS1, DS2, and DS3 **(A,B,C)**, and AIC$_C$ values for the fits **(D,E,F)**, respectively.

Unfortunately, the only regional data available are the value for τ_{cr} of the solid clay bricks. It is worth noting that the infills in RC structures are made with cement mortar, especially in the Kathmandu Valley, where most of the RC buildings are concentrated (e.g., Chaulagain et al., 2016b; Giordano et al., 2020a).

Data from 24 shear tests on solid brick masonry with cement mortar, selected among a collection of data provided by NSET (NSET, 2017) and gathered during the EPSRC SAFER project (http://www.safernepal.net/), are employed here to demonstrate a methodological application of regionalisation of FAST input properties. The same fitting procedure used in the previous section was applied to this new regional data (see **Figure 6A**)). The AIC$_C$ values for the distributions (see **Figure 6B**) show that the Log-Normal is the best fit for the Nepalese data.

Because the Nepalese and global data are both Log-Normal, it is possible to use a closed-form solution for Bayesian updating of the global data (prior data) using the Nepalese tests as additional information (likelihood). The global data set (i.e., τ_{global}) is updated using **Eqs. 10–12** (Benjamin and Cornell, 1970; Ang and Tang, 1984), where $\mu log(G)$ and $\sigma log(G)$ are the mean and standard deviation of the logarithm of τ_{global} (i.e., the prior global data), respectively. $\mu log(N)$ and $\sigma log(N)$ are the mean and standard deviation of the logarithm of τ_{Nepal}, respectively; n_G is the number of data points for the global data set; and n_N is the number of the new Nepalese data. The results of **Eqs. 10, 12** are the posterior log-normal distribution parameters for τ_{cr} (i.e., $\tau_{Updated}$ in **Supplementary Material, Table S3**).

FIGURE 6 | (A) Distribution of Nepalese shear stress (τ_{Nepal}) and **(B)** AIC$_C$ comparison of the distributions.

FIGURE 7 | Comparison of Nepalese shear data to global shear data and updated data relative contribution of RC frame.

$$\mu log\,(B) = \frac{\mu log\,(G)\,n_G + \mu log\,(N)\,n_N}{n_G + n_N} \qquad (10)$$

$$s'' = \sqrt{\frac{\left((n_G-1)\sigma log\,(G)+n_G\mu log\,(G)^2\right)+\left((n_N-1)\sigma log\,(N)\right.}{\left.+n_N\mu log\,(N)^2\right)-(n_G+n_N)\mu log\,(B)}{n_G + n_N - 1}} \qquad (11)$$

$$\sigma log\,(B) = s'' \cdot \sqrt{\frac{n_G + n_N - 1}{2} \cdot \frac{\Gamma\left(\frac{n_G+n_N-3}{2}\right)}{\Gamma\left(\frac{n_G+n_N-2}{2}\right)}} \qquad (12)$$

The results of the Bayesian updating of the log-normal distribution for τ_{cr} are shown in **Figure 7**. The distribution for the Nepalese bricks is very similar to that of the global data set. This is probably because of the common use of cement mortar, but still, this can indicate a reasonably good practice for mixing

the cement mortar in Nepal. On the other hand, these tests do not necessarily represent the standard practice as they are a limited sample. For example, reconnaissance reports have shown different standards in the quality of mortars of infill walls in the same type of buildings (e.g., Build Change Org, 2015). The Bayesian updating affects also the standard deviation relative to the global data set.
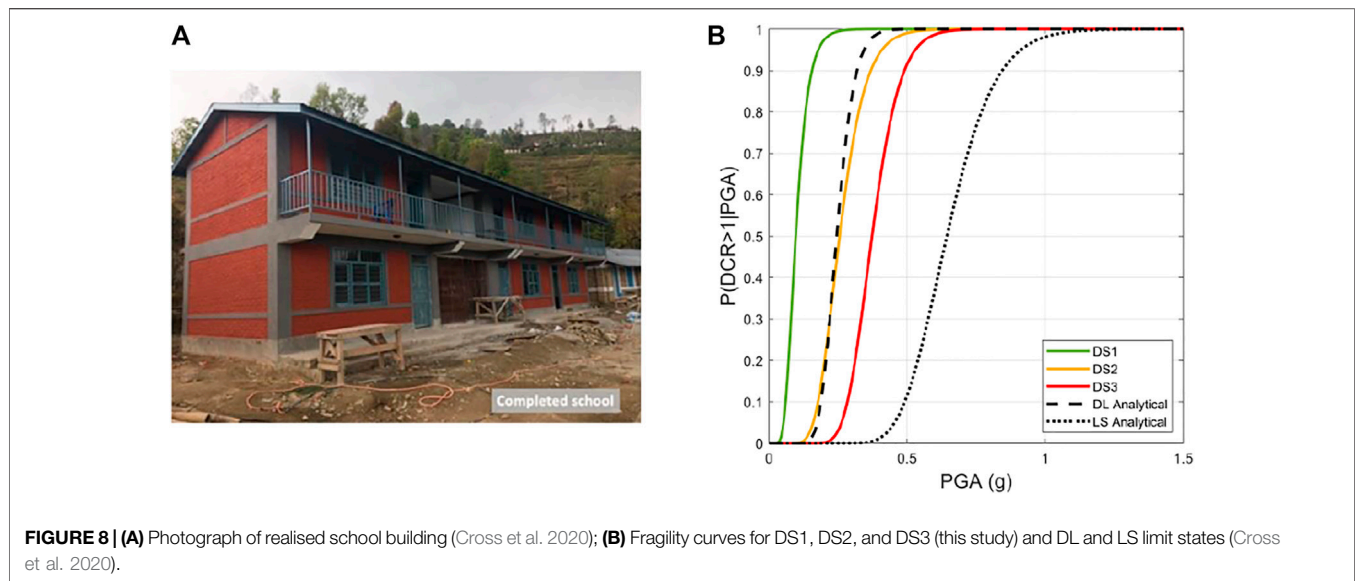
In addition to the modifications of the FAST method parameter of the shear strength, the overstrength parameter of the infills was also adapted to account for the presence of solid bricks. In particular, the CC equations (**Eqs. 4, 5**) presented by De Luca et al. (2015) have been modified for solid clay bricks, whereby the $\tau_{max} = 1.55\tau_{cr}$ instead of $\tau_{max} = 1.3\tau_{cr}$, as is used for hollow clay bricks (Blasi et al., 2018).

The relative contribution of RC frame to the lateral resistance at the peak lateral load (α) is commonly assumed to be 0.5 (De Luca et al., 2014). A more recent analytical assessment of RC buildings with masonry infills shows that the relative contribution of the RC frame decreases with a higher τ_{cr} value. This relationship is given in **Eq. 13** (Scala et al., 2020). It is shown in Scala et al. (2020) that this equation has a greater efficiency for τ_{cr} values between 0.27 and 0.47 MPa. However, it should be noted that with the assumed the second-order polynomial form, at a high τ_{cr} value, the alpha value starts to increase again (i.e., the contribution of RC would increase as the strength of infills increases). As this cannot be the case, at τ_{cr} values greater than 0.47 MPa, the α is set to 0.41, the polynomial minimum point. This recent result from the literature is employed herein to update the assumption in the FAST method application for the Nepalese context.

$$\alpha = \begin{cases} 2.70\tau_{cr}^2 - 2.57\tau_{cr} + 1.02 & \tau_{cr} \le 0.47\ MPa \\ 0.41 & \tau_{cr} > 0.47\ MPa \end{cases} \qquad (13)$$

Single Building Validation—Pahar Trust School

The FAST-NEPAL methodology is applied to a single RC building with masonry infills. The results were compared to the detailed

FIGURE 8 | (A) Photograph of realised school building (Cross et al. 2020); **(B)** Fragility curves for DS1, DS2, and DS3 (this study) and DL and LS limit states (Cross et al. 2020).
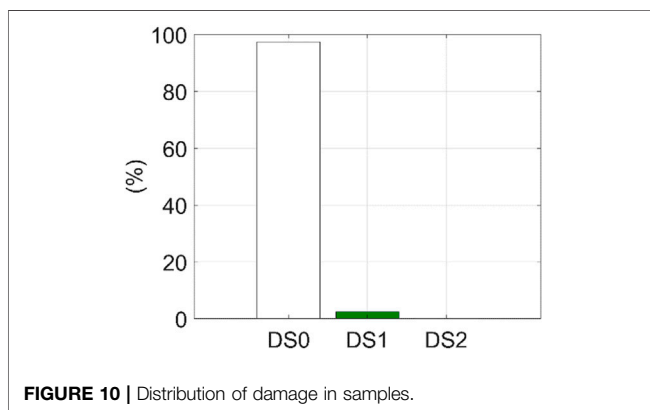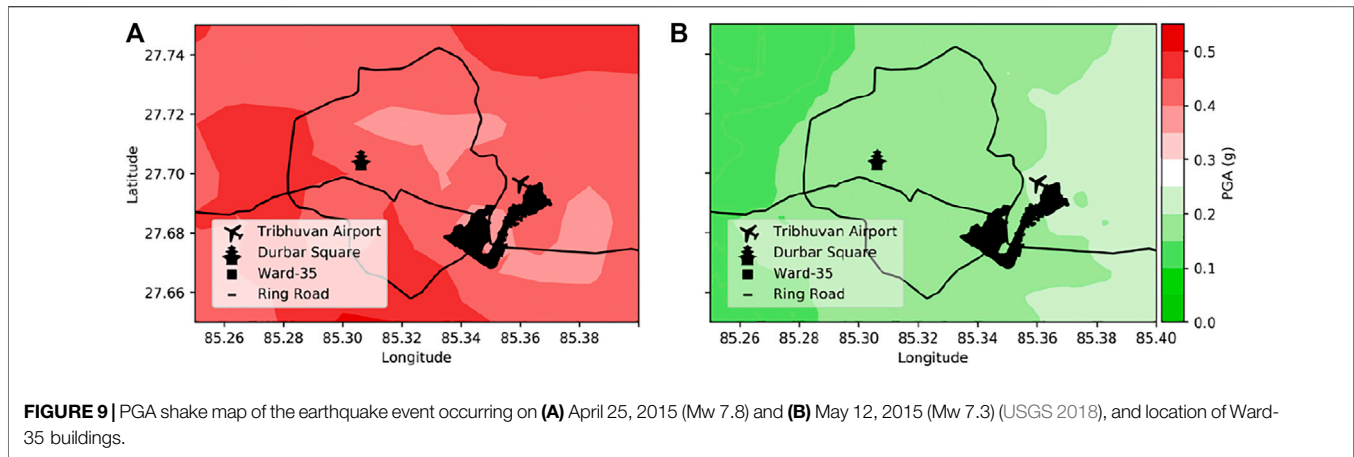
analytical assessment work previously carried out by Cross et al. (2020) to evaluate the validity of the FAST methodology as adapted according to the considerations provided in the previous sections. Pahar Trust is a United Kingdom–based charity that designs and builds RC schools with masonry infills across Nepal. Cross et al. (2020) used the non-linear time history analysis results on a Pahar Trust's school design to derive the fragility curves for the structure under damage limitation (DL) and life safety (LS) limit states. The school building has two storeys and is 4.9 m deep, 20.3 m wide, and 5.8 m tall. A photograph is shown in **Figure 8A**. Further details of the structural layout and materials can be found in Cross et al. (2020). In Cross et al. (2020), the DL limit state is defined at the IDR where all of the infills have exceeded their peak shear resistance (Ricci et al., 2016); this is found to be an IDR of 0.19%. The LS limit state is defined as 2.0% (ASCE/SEI 41-17, 2017).

The FAST methodology is applied using the updated Nepalese parameters. The building is assumed to be compliant with NBC 105 (1994), and therefore the design spectrum shown in **Figure 1A** is used. The available ductility, μ_s, is assumed to take a value of 3.13 as the building can be considered engineered. The IDR for DS1, DS2, and DS3 are assumed to be log normally distributed. The mean τ_{cr} value is assumed to be 0.05 MPa because this is the value used in Cross et al. (2020) and is from a regionalised material test on 1:6 cement–sand mortar, corresponding to that used in the school building. Using this τ_{cr} value allows a like-for-like comparison of the fragilities. The coefficient of variation of the τ_{cr} is assumed to be equal to that of the $\tau_{updated}$ dataset. The contribution of the RC frame at the peak lateral load (α) is assumed to correspond to the τ_{cr} distribution with **Eq. 13**. One hundred iterations were carried out in the Monte Carlo simulation to generate the fragility curves with FAST, and the mean fragility parameters were calculated for DS1, DS2, and DS3. It should be noted that the mean IDR for DS1,

DS2, and DS3 are 0.18%, 0.39%, and 1.01%, respectively, and the DL and LS limit state IDR from Cross et al. (2020) are 0.19% and 2.00%, respectively. These results can be seen in **Supplementary Material, Table S4**. It can be noted that the IDR for DL limit state lies between the means for DS1 and DS2, and the IDR for LS limit state exceeds DS3. **Figure 8B** shows the fragilities and the analytical fragilities of FAST methodology from Cross et al. (2020).

The fragility curves derived with the FAST-NEPAL methodology are expressed in terms of EMS-98 DSs (Grünthal, 1998), whereas the fragility by Cross et al. is expressed in terms of Eurocode conventional limit states; hence, the comparison needs to be supported by additional considerations even if this does not harm its informative value.

There is a robust matching between DS2 and DL limit state with a η value of 0.248 and 0.245 g. It should be noted that both DS2 and DL limit state represent the point at which the masonry infills degrade, and this shows the relative ability of FAST-NEPAL to capture the fragility at this stage through a suitable estimation of IDR2. It can be seen from **Figure 8B** that the FAST-NEPAL methodology gives a slightly larger β value, which is to be expected due to the higher level of variability in the FAST method caused by varying parameter values (τ_{cr}, IDR1, IDR2, and IDR3). The η value of the LS limit state (0.644 g) from Cross et al. (2020) substantially exceeds that of the DS3 from this study (0.366 g); this is the expected results because the LS limit state identifies the failure in the RC structural elements that are not captured by the FAST method. The parameters for each of the fragility curves in **Figure 8B** were summarised in **Supplementary Material, Table S5**. The results show that FAST-NEPAL provides fragility curves that are located in the correct relative positions with respect to those of the detailed study by Cross et al. (2020), providing preliminary support to the modifications made to assess the Nepalese RC-infilled buildings.

FIGURE 9 | PGA shake map of the earthquake event occurring on (A) April 25, 2015 (Mw 7.8) and (B) May 12, 2015 (Mw 7.3) (USGS 2018), and location of Ward-35 buildings.

FIGURE 10 | Distribution of damage in samples.

BUILDING PORTFOLIO VALIDATION—WARD-35 DATABASE

Gorkha 2015 Earthquake

On April 25, 2015, an earthquake of a magnitude (M_W) 7.8 struck Nepal at 06:11 a.m. UTM in the district of Lamjung in the Gandaki administrative zone, 77 km from the capital of Kathmandu (population of 1.5 million), causing 8,790 deaths and 22,300 injuries (Lizundia et al., 2017). The earthquake was followed by three aftershocks of M_W greater than 6.0 at 06:15 a.m. and 06:45 a.m. on April 25 and at 07:36 a.m. on April 26. Another significant event of M_W 7.3 occurred at 07:05 a.m. on May 12, 2015, followed by another aftershock of M_W 6.3 at 07:36 a.m. (Lizundia et al., 2016).

Figure 9 shows the PGA shake maps for the two main events (i.e., April 25 and May 12) according to USGS (2018) and the location of Ward-35 building data in Kathmandu provided by GENESIS Consultancy Pvt. Ltd. (2016). These shake maps are obtained on the basis of a single station recording located in the centre of Kathmandu (KATNP) and more than 200 km from the epicentre of the event. They do not provide a very detailed description of the shaking in the urban area of the city.

For the primary event (Figure 9A), the PGA that the buildings experienced varies across Ward-35, with the parts of the ward closer to the airport experiencing a lower PGA. For the second event (Figure 9B), the PGA that Ward-35 experienced is less variable according to the USGS shake map.
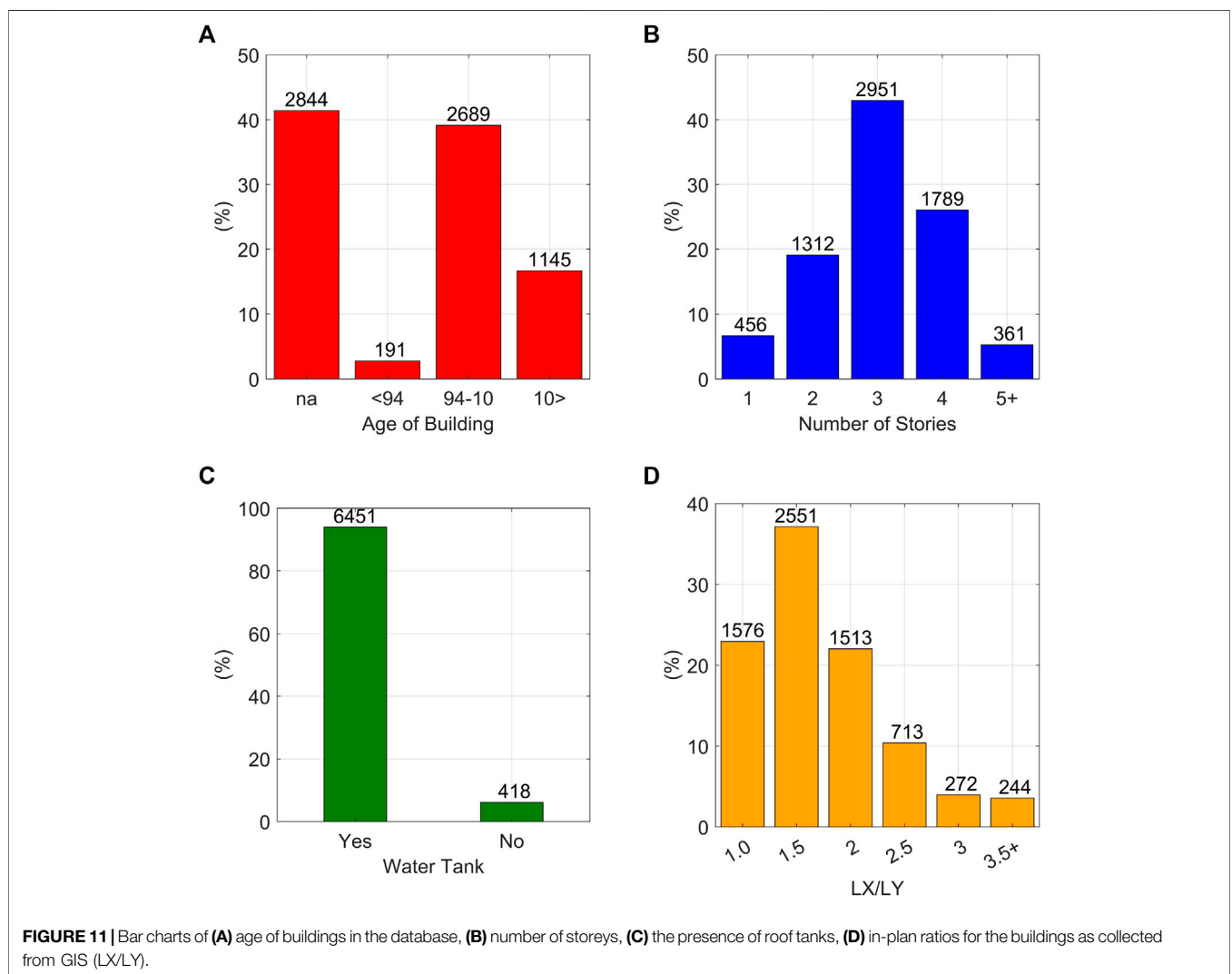
Building Database for Ward-35

The database of Ward-35 of Kathmandu is a collection of 6,869 RC frame buildings with masonry infills of fired clay brick. The database was assembled for cadastral and census purposes in Ward-35 of Kathmandu (GENESIS Consultancy Pvt. Ltd, 2016). The damage was graded using the EMS-98 grading system from photographic documentation available by a University of Bristol team working on the EPSRC project "Post-Natural Disaster downtime quantification after earthquakes through remote sensing: the case of the Mw 7.8 Gorkha 2015 (Nepal)", see the aggregated damage data in Figure 10 and the disaggregated data considering the number of storeys in Table 2. The data were collected by GENESIS Consultancy Pvt. Ltd. (2016) for the Nepalese government months after the 2015 earthquake and finalised in June 2016. This means that any significantly damaged or collapsed buildings were not included in the database (the database was assembled for census purposes and not for post-earthquake damage evaluation). The damage evaluation is based on the limited photographic documentation available for each building in the database, which is not highly reliable but still a useful preliminary test bed for the FAST-NEPAL method.

Ward-35 of Kathmandu did not suffer significant damage as shown by documentation collected in post-earthquake reconnaissance reports (e.g., Goda et al., 2015; Gautam and Chaulagain, 2016; Build Change Org, 2015; Gautam et al., 2016; Lizundia et al., 2016; Shakya and Kawan, 2016; Lizundia et al., 2017). Most of the buildings are of recent construction, with 16% of building built since 2010 when the new NBC was released with advice on improved construction practice. Almost 40% of the buildings in the database were constructed between 1994 and 2010. This means they were built after the release of NBC 1994 Rules of Thumb. Only 2.8% of the buildings surveyed were built before 1994. However, more than 40% of the buildings could not have their age determined (i.e., na indicating not available age information), as shown in Figure 11A. GENESIS Consultancy Pvt. Ltd. collected information on the age of construction, the
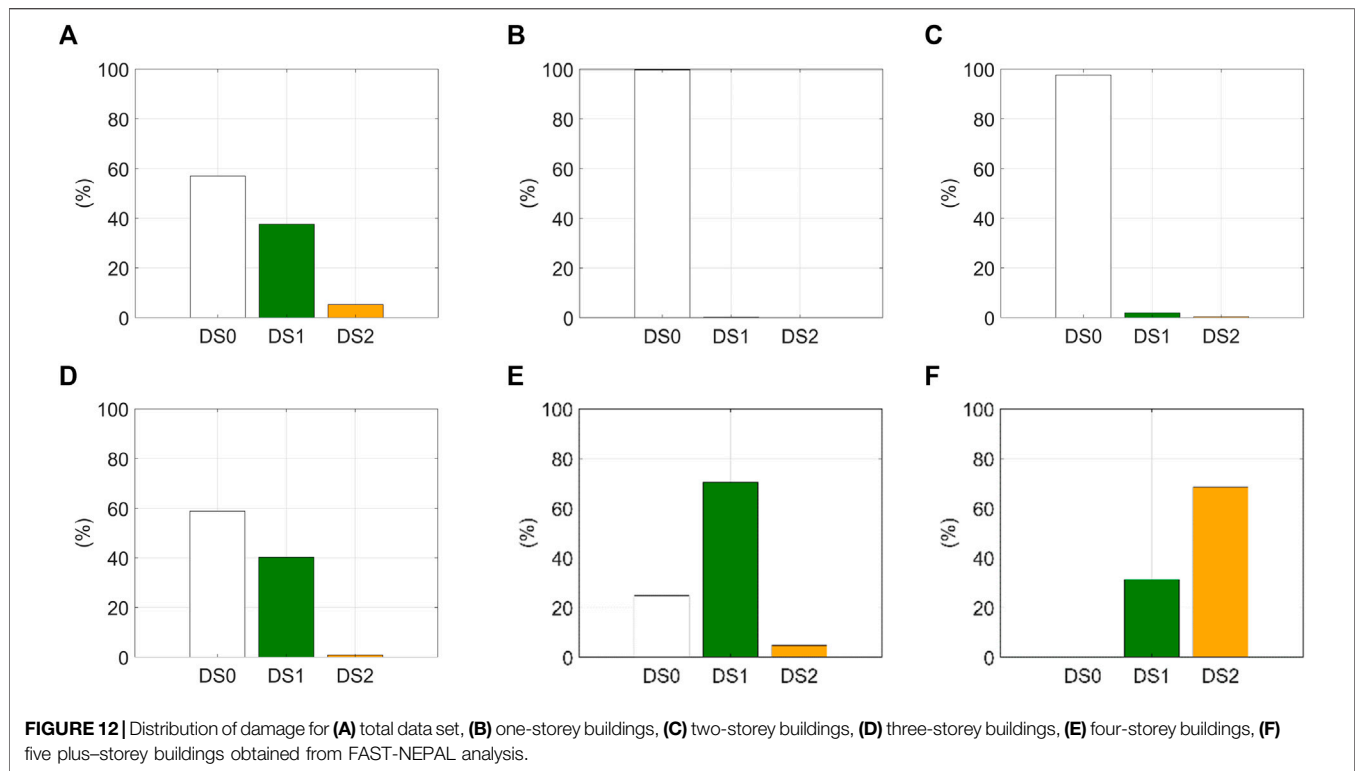
TABLE 2 | Damage state by building height using FAST-NEPAL for Ward-35 buildings.

Class	Number of buildings	FAST or observed	DS0 [#]	DS0 [%]	DS1 [#]	DS1 [%]	DS2 [#]	DS2 [%]
RC total	6,869	FAST	3,919	57.05	2,585	37.63	364	5.30
		Observed	6,693	97.43	172	2.504	11	0.160
1-Storey	456	FAST	455	99.78	1	0.22	0	0
		Observed	441	96.71	14	3.070	1	0.219
2-Storey	1,312	FAST	1,281	97.63	26	1.98	5	0.38
		Observed	1,267	96.57	42	3.201	3	0.229
3-Storey	2,951	FAST	1,736	58.86	1,186	40.21	27	0.91
		Observed	2,874	97.39	73	2.474	4	0.136
4-Storey	1789	FAST	445	24.87	1,259	70.37	85	4.75
		Observed	1,757	98.21	31	1.733	1	0.056
>5-Storey	361	FAST	1	0.27	113	31.30	247	68.4
		Observed	354	98.06	6	1.66	1	0.28

FIGURE 11 | Bar charts of (A) age of buildings in the database, (B) number of storeys, (C) the presence of roof tanks, (D) in-plan ratios for the buildings as collected from GIS (LX/LY).

number of storeys (**Figure 11B**), and the presence of roof tanks (**Figure 11C**) that can affect the vulnerability of the structure significantly, as seen in many post-earthquake reports (e.g., Shakya and Kawan, 2016). The ratio in-plan (LX/LY) for each building (i.e., the shape factor of the circumscribing rectangular shape around the building footprint) is obtained from the

FIGURE 12 | Distribution of damage for **(A)** total data set, **(B)** one-storey buildings, **(C)** two-storey buildings, **(D)** three-storey buildings, **(E)** four-storey buildings, **(F)** five plus–storey buildings obtained from FAST-NEPAL analysis.

database in ArcGIS and is shown in **Figure 11D**. LX/LY is a fundamental variable used in the FAST method (De Luca et al., 2017).
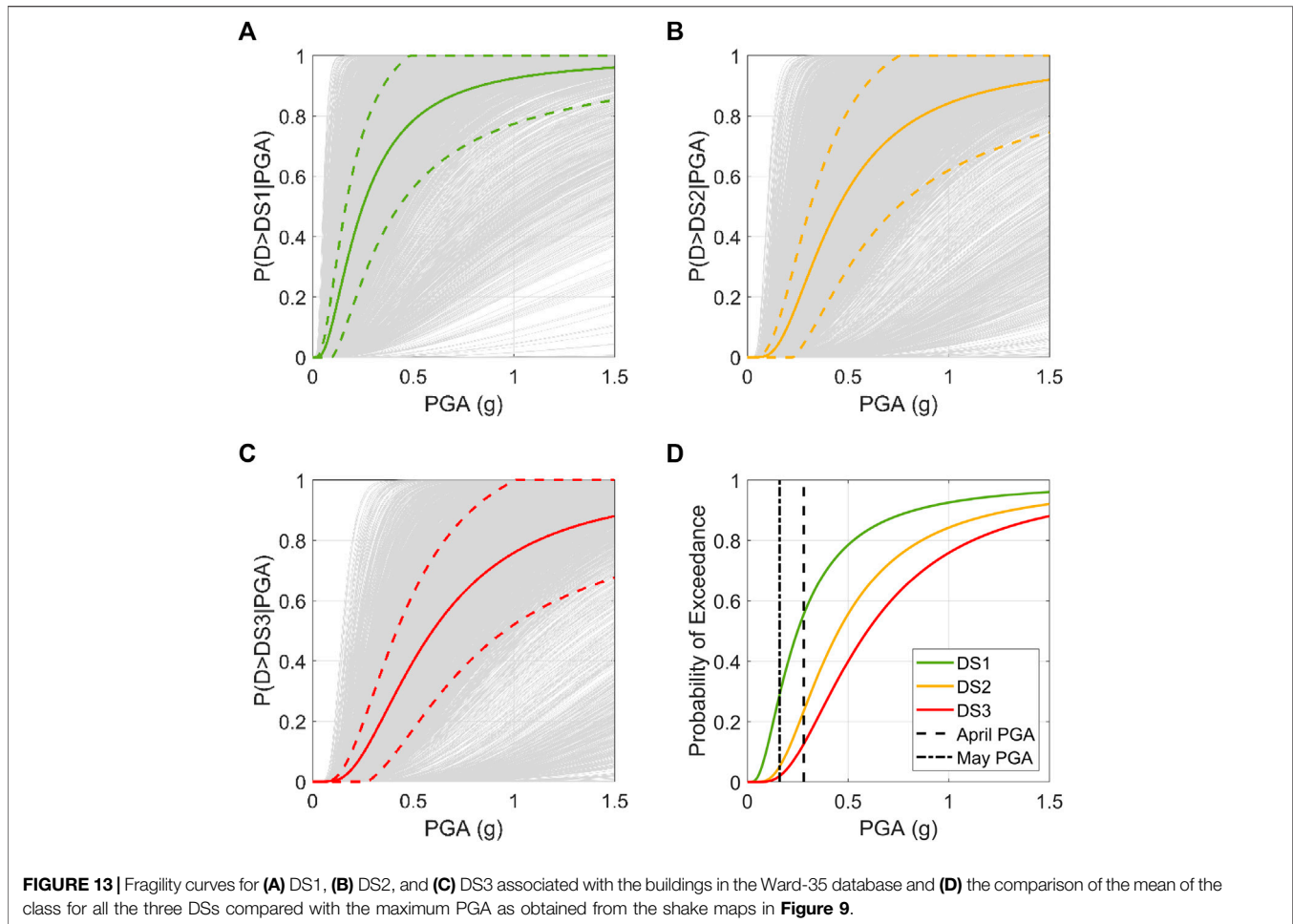
The buildings range in height from one storey to 11 storeys, with 70% being three to four storeys. This matches well with the number of storeys for which the FAST method was previously calibrated (De Luca et al., 2015) and other sources for Nepal such as Chaulagain et al. (2015), which report a similar range of heights.

According to the World Housing Encyclopedia (Marhatta et al., 2007), most buildings in Nepal are square or rectangular in plan. This matches the data in **Figure 11D**, with 82% having an in-plan ratio of 1–2. Databases such as De Luca et al. (2015), used to calibrate the FAST method in the Southern European area, are predominantly square or rectangular. The Nepalese buildings often have large balconies, which may mean that these ratios seem smaller than they are. Only 130 (1.9%) of the buildings are classified as having "soft storeys", but this datum was not used because the GENESIS Consultancy Pvt. Ltd. database of Ward-35 did not allow a strict structural interpretation of this condition; i.e., to distinguish between soft-storey configuration only in the front side of the building or full pilotis configuration (e.g., Kappos et al., 2006; Verderame et al., 2011). Of much more significant concern is that 94% of the buildings had roof water tanks (see **Figure 11C**). These tanks cause large increases in the building mass on the highest level. Their supports are typically not earthquake resistant and are unaccounted for in the building design stage. As the water tank volume is not quantified, it is impossible to account for this in the FAST-NEPAL methodology, but it is worth noting that an increase of the average building mass could be considered when more detailed information are available, especially for structures with a small surface where the relative mass contribution of the tank can be significant.

APPLICATION OF FAST-NEPAL TO WARD-35 OF KATHMANDU

The FAST-NEPAL methodology is then applied to the building database for Ward-35 of Kathmandu. As the Mandatory Rules of Thumb introduced in 2010 (UNDP, 2010) did not affect the design spectrum of the NBC 105 (1994), the $S_{a,d}(T)$ is assumed equal to 0.08 g for all buildings. The value of R_α (the structural redundancy factor) and R_ω (the over-strength material factor) were taken, respectively, equal to 1.0 and 1.0 for buildings where the age was not available (na in **Figure 11A**) and pre-1994 buildings (no-code buildings). R_α and R_ω were taken, respectively, equal to 1.0 and 1.45 for 1994–2010 buildings. This assumption considers the steel overstrength guaranteed by industrial quality control (IS 456, 1978; De Luca et al., 2014; Galasso, 2014). After 2010, 1.1 and 1.45 are used for R_α and R_ω, respectively, due to the release of the Nepal Department of Urban Development and Building Construction (UNDP, 2010) guidelines and a greater degree of code compliance. In addition, 1.1 is the R_α used in previous FAST studies (De Luca et al., 2014) and based on Borzi and Elnashai (2000). The Monte Carlo simulation was run for 100 iterations for each building with the variable parameters being τ_{cr}, α, DS1, DS2, and DS3. The Monte Carlo simulation results on each building were used to determine a fragility curve for each building in the database.

FIGURE 13 | Fragility curves for **(A)** DS1, **(B)** DS2, and **(C)** DS3 associated with the buildings in the Ward-35 database and **(D)** the comparison of the mean of the class for all the three DSs compared with the maximum PGA as obtained from the shake maps in **Figure 9**.

Comparison With Damage Data

The FAST analysis was performed for each of the structures, with the mean value of the 100 iterations being taken to define the required PGA to exceed a specific DS for each particular building. The DS for each of the structures in response to the April 2015 Gorkha earthquake can then be computed (see in **Table 2** and **Figure 12**). These values can be directly compared to the observed DSs shown in **Table 2**. The buildings that have exceeded DS3 have not been separated from those that exceeded DS2. This is because the Ward-35 database did not include any building exceeding DS3. Therefore, to allow a direct comparison of results, data up to the exceedance of DS2 have been considered for comparison. As expected, the comparison of a large-scale analytical approach such as FAST with observational data shows that the FAST-NEPAL methodology tends to overestimate the level of damage of the buildings. This is particularly evident in structures of four storeys or more. This is due to some of the conservative assumptions that are made in the FAST-NEPAL methodology. However, the method still accurately captures the dominance of DS0.

Comparing the observed and FAST values in **Table 2** for the ≥5-storey class, FAST-NEPAL predicts that the number of buildings in DS1 and in DS2 is 113 and 247, respectively. This is greater than the actual numbers of 6 for DS1 and 1 for DS2. For four-storey buildings, the FAST method predicted 655 buildings for DS1 and 38 for DS2. This was an overestimate because the database had 31 buildings exceeding DS1 and one building exceeding DS2. FAST tends to underestimate damage for lower number of storeys, as can be seen comparing the values for the one-storey and two-storey classes. This underestimate is likely caused by the fact that FAST cannot account for the differences in compliance with codes and good practices for a single-storey building compared with a multiple-storey building. The latter trend has some counterparts in Mediterranean practice. This explains the general phenomenon that analytical approaches underestimate the vulnerability of one-storey buildings and overestimate that of multiple-storey buildings (e.g., De Luca et al., 2017).

Fragility Curves FAST-NEPAL

Fragility curves were obtained through Monte Carlo simulation with $\tau_{Updated}$, IDR1, IDR2, IDR3, and α varying for each iteration of each building of the data set. The Monte Carlo simulation ran 100 iterations for each building, and then the fragilities were

obtained for DS1, DS2, and DS3. For each DS, the mean (μ) and the mean ± one standard deviation (σ) were obtained as shown in **Figure 13**. In **Figure 13D**, the mean fragilities for the three DSs are represented together for all the data sets. The fragilities are also compared with the PGA values for the May 12 (0.16 g) and April 25 (0.28 and 0.32 g) Gorkha earthquakes (see **Figure 9**). The value of 0.28 g for April 25 is represented in **Figure 13D**. The results obtained account implicitly for the predominant design approach observed in Ward-35, and they reflect the differences in design as assumed in Section 6.1.

Recent PSHA studies carried out by Stevens et al. (2018) have shown that Ward-35 has a 475-year return period earthquake (10% probability in 50 years) of 0.64 g. This would lead to a 45% probability of exceeding DS3, a 60% probability of exceeding DS2, and an 80% probability of exceeding DS1. Because of the conservative nature of some of the assumptions of the FAST methodology, this can be considered a worst-case scenario. The design value of PGA for 10% probability in 50 years in Kathmandu according to the 2020 Nepalese code (NBC 105, 2020) is 0.35 g. This value is somewhat lower than the value provided by Stevens et al. (2018). This is likely caused by different assumptions for the Ground Motion Prediction Equations used for the different studies and social and political considerations about seismic design implementation in the country to improve resilience and best practice.

Giordano et al. (2020b) used data from the Structural Integrity and Damage Assessment of approximately 18,000 school buildings across Nepal, assembled by the World Bank, to derive empirical fragilities. These fragilities are separated on the basis of structural typology and carried out using a Bayesian updating procedure. The damage data collected by the World Bank used a damage scale that can be assimilated to the EMS-98 scale (Grünthal, 1998) similarly to this study and geolocated all around Nepal. Fragility curves for DS1 are not given. Giordano et al. (2020b) gives a η value of 0.19 g for DS2 compared with the aggregated data for Ward-35, which gives a value of 0.49 g (see **Figure 13D**). This discrepancy is due to a lower quality of building control found in more rural parts of Nepal from which most of the data from Giordano et al. are located. For DS3, Giordano et al. (2020b) gives a η value of 0.27 g compared with this study, which gives a value of 0.62 g (see **Figure 13D**). This difference can again be attributed to the difference in construction quality. It should also be noted that the buildings in Ward-35 are relatively new, with 55.8% of the buildings being constructed since 1994. This would result in these buildings being designed to a higher standard than the school buildings from across Nepal.

CONCLUSION

In this work, the spectral-based FAST method is modified for the regional case of Nepal. A comparison is then carried out using numerical fragilities from Cross et al. (2020). Then, damage data relating to RC-infilled buildings in Ward-35 of Kathmandu are used as a test bed to validate the new FAST-NEPAL method. Damage data from Ward-35 are not the best possible benchmark for the Nepal version of FAST due to the data collection not being carried out immediately after the

event. However, the database provides preliminary insights into the accuracy and application of the methodology in Nepal.

The FAST method has previously been calibrated for European seismic events using direct damage comparison with field data (De Luca et al., 2014; Manfredi et al., 2014; De Luca et al., 2017) and fragility curves (De Luca et al., 2015). The main advantage of the method is the possibility to use several parameters calibrated from experimental data to account for the regional characteristics of buildings. The analysis can be performed quickly, avoiding any Finite Element modeling of the building or of the archetype representing a building class. The method in its current version accounts for up to DS3, which is considered suitable for rapid loss assessment and repair/retrofitting in the aftermath of an earthquake event.

In this study, the FAST methodology was modified for the Nepalese case using local data of the shear cracking strength (τ_{cr}) and updating the prior Log-Normal distribution to get an updated distribution for τ_{cr}. The IDR for DS1, DS2, and DS3 were updated on the basis of data from Cardone and Perrone (2015). The available ductility (μ_s) was updated using analytical pushover analyses on Nepalese RC with masonry infill buildings from Chaulagain (2016a) with the assigned μ_s value varying on the basis of the age of the building (and therefore likelihood of it being considered as "engineered"). Finally, the relative contribution of the RC frame to the lateral resistance at the peak lateral load (α) was updated using recent work on the relationship between τ_{cr} and α (Scala et al., 2020).

The Nepalese version of the FAST methodology was applied to a two-storey RC with infill building from Cross et al. (2020). All the modified parameters listed above were used except for the τ_{cr} where the value from Cross et al. (2020) was used to allow a like-for-like comparison. The results showed a strong level of matching (0.248 and 0.245 g) between the damage-limitation limit state and DS2, representing the point at which the masonry infills degrade.

The Nepalese version of the FAST methodology was then applied to the building database for Ward-35 of Kathmandu. The FAST method accurately captured the dominance of DS0 but overestimated the observed level of damage. This could be due to the conservative nature of FAST methodology and the low accuracy of damage data from photographic evidence. The FAST method overestimated the level of damage for one and two-storey structures. This is a common occurrence for analytical approaches (De Luca et al., 2017) and can be attributed to smaller buildings being less likely to be code conforming.

DATA AVAILABILITY STATEMENT

The original contributions presented in the study are included in the article/**Supplementary Material**; further inquiries can be directed to the corresponding author. Supporting data for this study are from third party sources. All data produced in this study are provided in full within this paper.

AUTHOR CONTRIBUTIONS

All authors contributed to the conception of the study. TC developed the final version of the MATLAB code for the FAST-NEPAL method and produced the figures. GW developed an early version of the FAST-NEPAL code as part of his undergraduate studies. All other authors contributed to writing and reviewing the paper.

ACKNOWLEDGMENTS

SUPPLEMENTARY MATERIAL

The Supplementary Material for this article can be found online at: https://www.frontiersin.org/articles/10.3389/fbuil.2021.689921/full#supplementary-material

REFERENCES

Abrams, D. P. (1992). June. Safe Limits for Lateral Capacity of Cracked URM walls. *Proc. 6th Can. Masonry Symp.* 1, 235–246.

Akaike, H. (1974). A New Look at the Statistical Model Identification. *IEEE Trans. Automat. Contr.* 19 (6), 716–723. doi:10.1109/tac.1974.1100705

Akehashi, H., and Takewaki, I. (2019). Optimal Viscous Damper Placement for Elastic-Plastic MDOF Structures under Critical Double Impulse. *Front. Built Environ.* 5, 20. doi:10.3389/fbuil.2019.00020

Andreaus, U., and Moroder, M. (1991). *Stato dell'arte sui legami costitutivi dei solidi murari.*

Ang, A. H. S., and Tang, W. H. (1984). *Probability Concepts in Engineering Planning and Design.* in *Decision, Risk, and Reliability*, Vol. 2. NEW YORK, NY 10158, USA: JOHN WILEY & SONS, INC., 605 THIRD AVE., 608.

ASCE/SEI 41-17 (2017). *Seismic Evaluation and Retrofit of Existing Buildings.* Reston, VA: American Society of Civil Engineers.

Augenti, N., Parisi, F., and Acconcia, E. (2012). "MADA: Online Experimental Database for Mechanical Modelling of Existing Masonry Assemblages," in Fifteenth World Conference on Earthquake Engineering.

Benjamin, J. R., and Cornell, C. A. (1970). *Probability, Statistics, and Decision for Civil Engineers.* Mineola, New York: Dover Publications, Inc.

Blasi, G., De Luca, F., and Aiello, M. A. (2018). Brittle Failure in RC Masonry Infilled Frames: The Role of Infill Overstrength. *Eng. Structures* 177, 506–518. doi:10.1016/j.engstruct.2018.09.079

Blasi, G., De Luca, F., Perrone, D., Greco, A., and Antonietta Aiello, M. (2021). MID 1.1: Database for Characterization of the Lateral Behavior of Infilled Frames. *J. Struct. Eng.* 147 (10), 04721007.

Borzi, B., and Elnashai, A. S. (2000). Refined Force Reduction Factors for Seismic Design. *Eng. Structures* 22 (10), 1244–1260. doi:10.1016/s0141-0296(99)00075-9

Brando, G., Rapone, D., Spacone, E., O'Banion, M. S., Olsen, M. J., Barbosa, A. R., et al. (2017). Damage Reconnaissance of Unreinforced Masonry Bearing wall Buildings after the 2015 Gorkha, Nepal, Earthquake. *Earthquake Spectra* 33 (1_Suppl. l), 243–273. doi:10.1193/010817EQS009M

Build Change Org (2015). Nepal Earthquake Reconnaissance Report. Available at: http://www.buildchange.org/locations/nepal/ (version October 2015 last accessed September, 2020).

Caliò, I. (2011). La prova di scorrimento con martinetto piatto. Proceedings of the XIV ANIDIS. *Ital. Nacional Assoc. Earthquake Engineering),* 157. doi:10.1193/010817eqs009m

Cardone, D., and Perrone, G. (2015). Developing Fragility Curves and Loss Functions for Masonry Infill walls. *Earthquakes and Structures* 9 (1), 257–279. doi:10.12989/eas.2015.9.1.257

Cavanaugh, J. E. (1997). Unifying the Derivations for the Akaike and Corrected Akaike Information Criteria. *Stat. Probab. Lett.* 33, 201–208. doi:10.1016/s0167-7152(96)00128-9

CEN (2004). *Eurocode 8: Design of Structures for Earthquake Resistance. Part 1: General Rules, Seismic Actions and Rules for Buildings.* Brussels: Comité Européen de Normalisation. European standard EN1998-1:2004.

Centre Bureau of Statistics (CBS) (2012). *National Report, National Planning Commission Secretariat.* Kathmandu, Nepal: Central Bureau of Statistics.

Chaulagain, H., Rodrigues, H., Silva, V., Spacone, E., and Varum, H. (2016b). Earthquake Loss Estimation for the Kathmandu Valley. *Bull. Earthquake Eng.* 14 (1), 59–88. doi:10.1007/s10518-015-9811-5

Chaulagain, H., Rodrigues, H., Silva, V., Spacone, E., and Varum, H. (2015). Seismic Risk Assessment and hazard Mapping in Nepal. *Nat. Hazards* 78 (1), 583–602. doi:10.1007/s11069-015-1734-6

Chaulagain, H., Rodrigues, H., Spacone, E., and Varum, H. (2014a). Design Procedures of Reinforced concrete Framed Buildings in Nepal and its Impact on Seismic Safety. *Adv. Struct. Eng.* 17 (10), 1419–1442. doi:10.1260/1369-4332.17.10.1419

Chaulagain, H., Rodrigues, H., Spacone, E., and Varum, H. (2016a). Seismic Safety Assessment of Existing Masonry Infill Structures in Nepal. *Earthq. Eng. Eng. Vib.* 15 (2), 251–268. doi:10.1007/s11803-016-0320-6

Colangelo, F. (2012). A Simple Model to Include Fuzziness in the Seismic Fragility Curve and Relevant Effect Compared with Randomness. *Earthquake Engng Struct. Dyn.* 41, 969–986. doi:10.1002/eqe.1169

Cross, T., De Luca, F., De Risi, R., Ranamagar, T. R., Mitchell, T., and Sweetman, A. (2020). Mapping the Seismic Safety of RC "template Schools" in Nepal. *Int. J. Disaster Risk Reduction* 51, 101844. doi:10.1016/j.ijdrr.2020.101844

De Luca, F., Vamvatsikos, D., and Iervolino, I. (2013). Near-optimal Piecewise Linear Fits of Static Pushover Capacity Curves for Equivalent SDOF Analysis. *Earthquake Engng. Struct. Dyn.* 42 (4), 523–543. doi:10.1002/eqe.2225

De Luca, F., Verderame, G. M., Gómez-Martínez, F., and Pérez-García, A. (2014). The Structural Role Played by Masonry Infills on RC Building Performances after the 2011 Lorca, Spain, Earthquake. *Bull. Earthquake Eng.* 12 (5), 1999–2026. doi:10.1007/s10518-013-9500-1

De Luca, F., Verderame, G. M., and Manfredi, G. (2015). Analytical versus Observational Fragilities: the Case of Pettino (L'Aquila) Damage Data Database. *Bull. Earthquake Eng.* 13 (4), 1161–1181. doi:10.1007/s10518-014-9658-1

De Luca, F., Woods, G. E., Galasso, C., and D'Ayala, D. (2017). RC Infilled Building Performance against the Evidence of the 2016 EEFIT Central Italy post-earthquake Reconnaissance mission: Empirical Fragilities and Comparison with the FAST Method. *Bull. Earthquake Eng.,* 1–27. doi:10.1007/s10518-017-0289-1

Dizhur, D., Dhakal, R. P., Bothara, J., and Ingham, J. (2016). *Building Typologies and Failure Modes Observed in the 2015 Gorkha (Nepal) Earthquake,* 49. doi:10.5459/bnzsee.49.2.211-232No. 2 Response

EN (1996-3). *Eurocode 6 - Design of Masonry Structures - Part 3: Simplified Calculation Methods for Unreinforced Masonry Structures,* 2006. London: European Standard.

Erdik, M., and Fahjan, Y. (2008). "Damage Scenarios and Damage Evaluation," in *Assessing and Managing Earthquake Risk* (Dordrecht: Springer), 213–237.

Fajfar, P., and Gašperšič, P. (1996). The N2 Method for the Seismic Damage Analysis of RC Buildings. *Earthquake Engng. Struct. Dyn.* 25 (1), 31–46. doi:10.1002/(sici)1096-9845(199601)25:1<31:aid-eqe534>3.0.co;2-v

Galasso, C. (2014). *Probabilistic Analysis of Flexural Overstrength for New Designed RC Beams*. in *Second European Conference on Earthquake Engineering*.

Gautam, D., and Chaulagain, H. (2016). Structural Performance and Associated Lessons to Be Learned from World Earthquakes in Nepal after 25 April 2015 (MW 7.8) Gorkha Earthquake. *Eng. Fail. Anal.* 68, 222–243. doi:10.1016/j.engfailanal.2016.06.002

Gautam, D., Rodrigues, H., Bhetwal, K. K., Neupane, P., and Sanada, Y. (2016). Common Structural and Construction Deficiencies of Nepalese Buildings. *Innov. Infrastruct. Solut.* 1 (1), 1. doi:10.1007/s41062-016-0001-3

GENESIS Consultancy Pvt. Ltd. (2016). *Consultancy Services for Urban Base Map and Integrated Municipal GIS of Kathmandu Metropolitan City*. Ward No -35. Available upon request to the University of Bristol data repository. Shree Da Ram Prajapati.

Giordano, N., De Luca, F., and Sextos, A. (2020a). Analytical Fragility Curves for Masonry School Building Portfolios in Nepal. *Bull. Earthquake Eng.* 19 (2), 1121–1150. doi:10.1007/s10518-020-00989-8

Giordano, N., De Luca, F., Sextos, A., Ramirez Cortes, F., Fonseca Ferreira, C., and Wu, J. (2020b). Empirical Seismic Fragility Models for Nepalese School Buildings. *Nat. Hazards* 105 (1), 339–362. doi:10.1007/s11069-020-04312-1

Goda, K., Kiyota, T., Pokhrel, R. M., Chiaro, G., Katagiri, T., Sharma, K., et al. (2015). The 2015 Gorkha Nepal Earthquake: Insights from Earthquake Damage Survey. *Front. Built Environ.* 1, 8. doi:10.3389/fbuil.2015.00008

Grünthal, G. (1998). *European Macroseismic Scale 1998*. Luxembourg: European Seismological Commission (ESC).

IS:4326 (1976). *Earthquake Resistant Design and Construction of Buildings—Code of Practice*. New Delhi: Bureau of Indian Standards.

IS:456 (1978). *Indian Standard Code of Practice for plain and Reinforced concrete—Code of Practice*. New Delhi: Bureau of Indian Standards.

Kappos, A. J., Panagopoulos, G., Panagiotopoulos, C., and Penelis, G. (2006). A Hybrid Method for the Vulnerability Assessment of R/C and URM Buildings. *Bull. Earthquake Eng.* 4 (4), 391–413. doi:10.1007/s10518-006-9023-0

Kappos, A. J. (2000). "Seismic Design and Performance Assessment of Masonry Infilled RC Frames," in Proceeding of the 12th World Conference on Earthquake January 30th – February 4th Auckland (New Zealand. Paper id 989.

Lizundia, B., Davidson, R. A., Hashash, Y. M., and Olshansky, R. (2017). Overview of the 2015 Gorkha, Nepal. *Earthquake Earthquake Spectra Spec. Issue Earthquake Spectra* 33 (S1), S1–S20. doi:10.1193/120817eqs252m

Lizundia, B., Shrestha, S. N., Bevington, J., Davidson, R., Jaiswal, K., Jimee, G. K., et al. (2016). *M7. 8 Gorkha, Nepal Earthquake on April 25th, 2015 and its Aftershocks EERI Earthquake Reconnaissance Team Report*.

Manfredi, G., Prota, A., Verderame, G. M., De Luca, F., and Ricci, P. (20142012). 2012 Emilia Earthquake, Italy: Reinforced concrete Buildings Response. *Bull. Earthquake Eng.* 12 (5), 2275–2298. doi:10.1007/s10518-013-9512-x

Manfredi, G., Ricci, P., and M Verderame, G. (2012). Influence of Infill Panels and Their Distribution on Seismic Behavior of Existing Reinforced concrete Buildings. *Open Construction Building Techn. J.* 6 (1). doi:10.2174/1874836801206010236

Marhatta, Y. B., Bothara, J. K., Magar, M. B., and Chapagain, G. (2007). *Report*. Housing Report Pillar Walaghar (URM Infilled RC Frame Buildings) (No. 145).

Meli, R. (1973). "June. Behavior of Masonry walls under Lateral Loads," in Fifth world conference on earthquake engineering.

NBC 201 (1994). Nepal National Building Code. Mandatory Rules of Thumb for Reinforced concrete Buildings with Masonry Infills. [ebook] Available at: http://www.dudbc.gov.np/uploads/default/files/30f57e54649ba9b6e03dbdef12929ea5.pdf (Accessed July 11, 2020).

NBC 105 (2020). *Nepal National Building Code. Seismic Design of Buildings in Nepal*, [ebook].

NBC 105 (1994). Nepal National Building Code. Seismic Design of Buildings in Nepal [ebook] Available at: http://www.dudbc.gov.np/uploads/default/files/c25f315ba97fe50b056e7803296704b5.pdf [Accessed July 11, 2020).

NSET Nepal National Society for Earthquake Technology (2017). *Data on Cement Mortar Test from NepalEPSRC SAFER Project 2017-2020*. Available upon equest to the University of Bristol data repository.

Parajuli, Y. K., Bothara, J. K, Dixit, A. M., Pradhan, J. P., and Sharpe, R. D. (2000). "Nepal Building Code-Need, Development Philosophy and Means of Implementation," in 12th World Conference on Earthquake Engineering (Auckland, New Zealand, January.

Porter, K., Kennedy, R., and Bachman, R. (2007). Creating Fragility Functions for Performance-Based Earthquake Engineering. *Earthquake Spectra* 23 (2), 471–489. doi:10.1193/1.2720892

Ricci, P., De Risi, M. T., Verderame, G. M., and Manfredi, G. (2016). Procedures for Calibration of Linear Models for Damage Limitation in Design of Masonry-Infilled RC Frames. *Earthquake Engng Struct. Dyn.* 45 (8), 1315–1335. doi:10.1002/eqe.2709

Riddington, J. R., and Jukes, P. (1994). *A Comparison between Panel, Joint and Code Shear Strength*. Calgary, Canada: Proc. 10th IBMaC, 1481–1490.

Scala, S., Ricci, P., Del Gaudio, C., Gómez-Martínez, F., and Verderame, G. (2020). "Simplified Analytical Methodologies for Seismic Fragility Assessment of RC Buildings with Infills," in 17th World Conference on Earthquake Engineering (Sendai: Sendai).

Shakya, M., and Kawan, C. K. (2016). Reconnaissance Based Damage Survey of Buildings in Kathmandu valley: An Aftermath of 7.8Mw, 25 April 2015 Gorkha (Nepal) Earthquake. *Eng. Fail. Anal.* 59, 161–184. doi:10.1016/j.engfailanal.2015.10.003

Stevens, V. L., Shrestha, S. N., and Maharjan, D. K. (2018). Probabilistic Seismic Hazard Assessment of Nepal. *Bull. Seismological Soc. America* 108 (6), 3488–3510. doi:10.1785/0120180022

United Nations (2017). Department of Economic and Social Affairs, Population Division. World Population Prospects: The 2017 Revision *Available at:* http://www.worldometers.info/world-population/nepal-population/.

United Nations Development Program (UNDP) (2010). *Recommendations for Construction of Earthquake Safer Buildings - Earthquake Risk Reduction and Recovery Preparedness Programme for Nepal*. Kathmandu, Nepal: Department of Urban Development and Building Construction.

USGS (2018). [online]. See. Reston: U.S. Geological Survey. Available at: https://www.usgs.gov/ (Accessed March 10, 2020).

Valluzzi, M. R., Tinazzi, D., and Modena, C. (2002). Shear Behavior of Masonry Panels Strengthened by FRP Laminates. *Construction Building Mater.* 16 (7), 409–416. doi:10.1016/s0950-0618(02)00043-0

Vamvatsikos, D., and Allin Cornell, C. (2006). Direct Estimation of the Seismic Demand and Capacity of Oscillators with Multi-Linear Static Pushovers through IDA. *Earthquake Engng Struct. Dyn.* 35 (9), 1097–1117. doi:10.1002/eqe.573

Vamvatsikos, D., and Cornell, C. A. (2002). Incremental Dynamic Analysis. *Earthquake Engng. Struct. Dyn.* 31 (3), 491–514. doi:10.1002/eqe.141

Verderame, G. M., De Luca, F., Ricci, P., and Manfredi, G. (2011). Preliminary Analysis of a Soft-Storey Mechanism after the 2009 L'Aquila Earthquake. *Earthquake Engng. Struct. Dyn.* 40 (8), 925–944. doi:10.1002/eqe.1069

World Bank (2020) *Available at:* https://data.worldbank.org/indicator/NY.GDP.PCAP.CD?end=2019&locations=NP&most_recent_value_desc=false&start=1960

World Bank Group (2016). *Solving the Puzzle Innovating to Reduce Risk*. Full report. June 2016. *Available at:* https://www.gfdrr.org/sites/default/files/solving-the-puzzle-report.pdf.

Yi, W. H., Oh, S. H., and Lee, J. H. (2004). "August. Shear Capacity Assessment of Unreinforced Masonry wall," in 13th World Conference on Earthquake Engineering, 1–12.

Zarri, F. (1992). Consolidamento delle murature di edifici antichi mediante iniezioni di malta. *Costruire in Laterizio* 25, 63–69.

Zhuge, Y., Corderoy, J., and Thambiratnam, D. (1996). Behavior of Unreinforced brick Masonry under Lateral (Cyclic) Loading. *TMS J.* 14 (2), 55–62.